Supporting Information for

Salinity Exchange between Seawater/Brackish water and Domestic Wastewater through Electrodialysis for Potable Water

AUTHOR NAMES: *Mourin Jarin, Zeou Dou, Haiping Gao, Yongsheng Chen[*], Xing Xie[*]*

AUTHOR ADDRESS: School of Civil & Environmental Engineering, Georgia Institute of Technology, 200 Bobby Dodd Way, Atlanta, GA, 30332, United States

[*]**Corresponding author:** Xing Xie, Email: xing.xie@ce.gatech.edu, Phone: 4048949723; Yongsheng Chen, Email: yongsheng.chen@ce.gatech.edu, Phone: 4048943089.

Content	#
Pages	18
Additional Text	3
Figures	11

Table of Contents

1. Additional Text

Supplemental Text 1. The operation of the SEE includes two phases. At the transition point from phase 1 to phase 2, the two streams reach the same salt concentration (C_0). For theoretical phase 1 energy generation, the calculation is based on the free energy of mixing using Eq. S1, where R_g is the universal gas constant, T is the absolute temperature, c_I and c_{II} are the initial solute concentrations for the Stream I and Stream II, and φ is the dilution ratio defined as V_d/V_c which we considered 1 for our case.(Ramon et al., 2011) For our default condition c_I and c_{II} were 0.6 M and 0.01 M.

$$\Delta E_{mix} = 2R_g T(c_I ln\frac{c_I(1+\varphi)}{c_I+\varphi c_{II}} + \varphi c_{II} ln\frac{c_{II}(1+\varphi)}{c_I+\varphi c_{II}}) \quad \text{Eq. S1}$$

The minimum energy consumption for desalination was calculated based on Eq. S2, where R_g is the ideal gas constant, T is the absolute temperature, γ is the water recovery rate (considered 50% in this system since the volumes of both Stream I and Stream II are initially equivalent), C_0 is the initial concentration of both Stream I and Stream II at the beginning of phase 2, C_{If} is the Stream I effluent concentration, and C_{IIf} is the Stream II effluent concentration. If we consider replacing C_0 with $(C_{If} + C_{IIf})/2$, Eq. S1 and Eq. S2 are the same, which is logical considering the salt transfer process (phase 2) is just the reverse of the previous spontaneous mixing (phase 1). Due to the water transfer observed within the SEE system, the theoretical minimal energy consumption was calculated using the endpoint effluent concentration of Stream I (final desalinated water produced). This final desalinated water concentration was used to obtain the theoretical effluent concentration of Stream II, and the midpoint of these 2 effluent concentration values was used to represent C_0 in each case. This point of equilibrium determined where phase 1 ended and phase 2 began. Ideally

the system would reach equilibrium at half the operating time *t*, but due to the overpotential and water transfer, the EG phase is observed to be shorter.

$$EC_{min} = 2R_gT\left\{\frac{c_0}{\gamma} ln\left[\frac{c_{If}}{c_0}\right] - c_{IIf} ln\left[\frac{c_{If}}{c_{IIf}}\right]\right\} \quad \text{Eq. S2}$$

The real energy generation and consumption were calculated based on Eq. S3, where I_c is constant current applied and V_{cell} is the voltage potential over time. Negative values correlated to energy generation, while positive values correlated to energy consumption. Due to the water leakage in the SEE system, the effluent concentrations were used similarly as in Eq. S2 to calculate the equilibrium midpoint.

$$EC = I_c \int_{t_0}^{t_f} V_{cell}(t)dt \quad \text{Eq. S3}$$

The energy generation efficiency for phase 1 is calculated by the fraction of real energy generated over the theoretical, while the energy consumption efficiency for phase 2 is calculated by the fraction of theoretical energy consumption over the real energy consumed. The energy consumption was calculated and normalized to the mols of ions transferred for each operating condition. After assessing the water leakage, the energy consumption was also normalized to the volume of treated water produced.

In electrodialysis systems not all the current is used effectively and back diffusion of ions or co-ion transport occurs due to imperfect membranes.(Turek, 2003) The coulombic efficiency is calculated as the total electric charge transported by ions over the electric charge transported applied to the system.(Galama et al., 2014) This was based on Eq. S4, where n is the moles of ions

transferred, F is the Faraday's constant of 96485 C/mol, I_c is constant current, and *t* is the operation time.

$$CE = \frac{nF}{I_c t} \quad \text{Eq. S4}$$

Supplemental Text 2. The conductivities of prepared NaCl feed solutions were all measured using a conductivity probe. These measured values were then converted from mS/cm to M using a standard curve (Figure S2). For the final conductivities, the measured values were corrected for their change in volume due to water transport. As the SEE cell holds an uncertain amount of leftover water at any point, conductivities were also corrected to limit any errors in manually measuring final water volume. In regards to Fig 2a, the measured and calculated values for conductivity, final volume, and salinity are presented in Table S1, along with the example calculations for how they were obtained in consistency with all other data in Eqs. S5, S6, and S7.

Table S1. Properties of the two streams before and after the SEE operation.

	Conductivity at t_0 (mS/cm)	Salinity at t_0 (g/L)	Conductivity at t_f (mS/cm)	Final Volume (L)	Corrected Conductivity at t_f (mS/cm)	Corrected Salinity at t_f (g/L)
Stream I	59.27	32.45	0.8748	0.176	0.7698	0.42
Stream II	1.278	0.70	57.44	0.226	64.91	35.54

$$\text{Salinity at } t_0 = 59.27\frac{mS}{cm} \times 0.00936 \frac{M}{\frac{mS}{cm}} \times 58.44\frac{g}{mol} = 32.45\frac{g}{L} \quad \text{Eq. S5}$$

$$\text{Corrected Conductivity at } t_f = \frac{(0.176L)\times\left(0.8748\frac{mS}{cm}\right)}{0.2L} = 0.7698\frac{mS}{cm} \quad \text{Eq. S6}$$

$$\text{Corrected Salinity at } t_f = 0.7698\frac{mS}{cm} \times 0.00936 \frac{M}{\frac{mS}{cm}} \times 58.44\frac{g}{mol} = 0.42\frac{g}{L} \quad \text{Eq. S7}$$

Supplemental Text 3. Electrodialysis is known to transport water along with ions during its process and consequently affect the efficiency of desalination and the amount of final water produced.(Wilson, 1960; Strathmann, 2004) This water transport occurs as either osmosis or electro-osmosis. Osmosis (free water transport) increases with osmotic pressure differences caused by the concentration gradient between concentrate and dilute.(Sata, 2007; Tedesco et al., 2016,2017) Electro-osmosis (transport of water bound to ions) occurs when ions pass through the membrane.(Mulder and Mulder, 1996; Tedesco et al., 2016,2017) Water transport can also be attributed to water molecules permeating due to a hydrostatic pressure gradient.(Tedesco et al., 2016,2017) The combination of osmosis and electro-osmosis can lead to significant water transport during the SEE process, limiting the decrease in the concentration of Stream I near the end of the process as water may transport proportionally with ions through the membrane.(Porada et al., 2018) Especially osmosis, can contribute to a lower dilute yield (desalinated water produced) as well as higher energy losses resulting from decreased electrical current used for the actual desalination process.(Brydges and Lorimer, 1983; Indusekhar and Krishnaswamy, 1985; Galama et al., 2014) The main methods to decrease the osmotic water transport in electrodialysis are by reducing the concentration gradient over the IEMs, increasing the current density of operation, and thus, decreasing the energy efficiency.(Porada et al., 2018) We attribute the water transport phenomenon to our results of lower than expected salinities in Stream II due to higher volume of water, and decreased desalinated water yield in Stream I.

2. Additional Figures

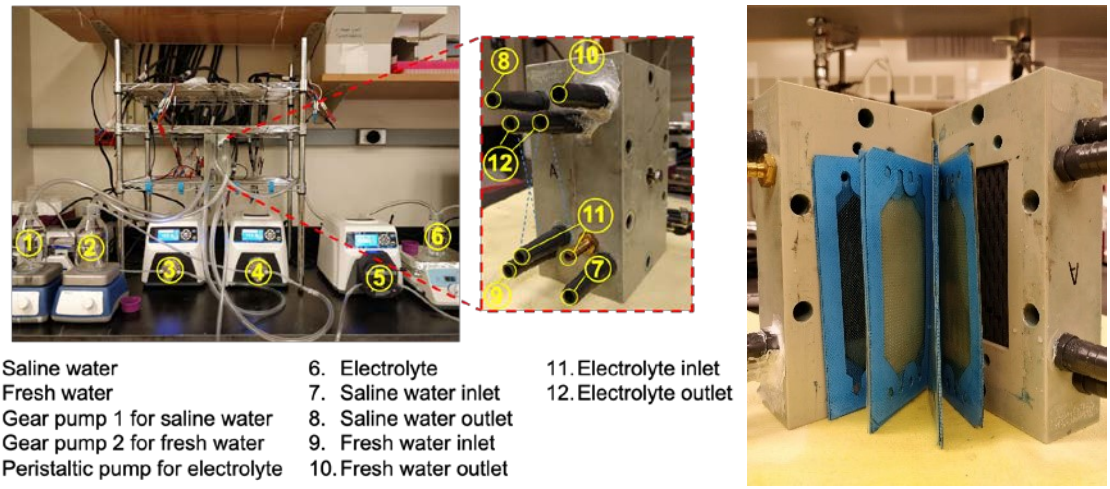

Figure S1. Experimental setup of the SEE system.

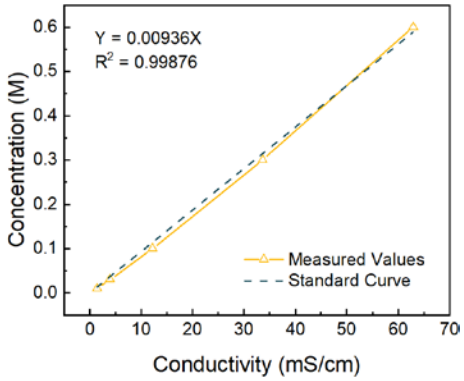

Figure S2. Standard curve to convert measured conductivity values to molarity of NaCl.

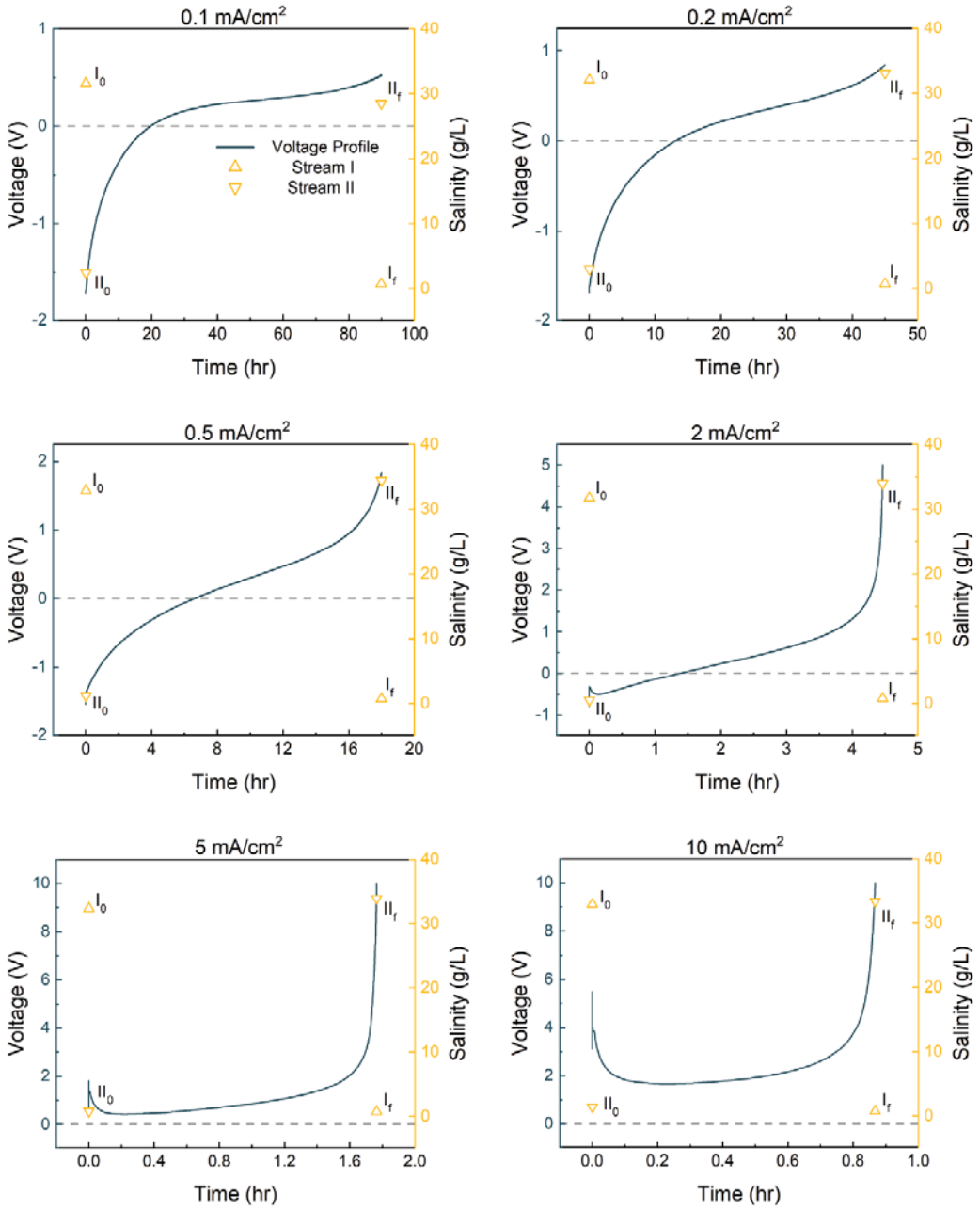

Figure S3. SEE operation with varying current densities. The operating conditions for varying applied current density were a feed solution flow rate of 200 mL/min, a Stream I NaCl concentration of 0.6 M, and a Stream II NaCl concentration of 0.01 M. The flow rate for the electrode rinse solution was fixed at 100 mL/min. Salinity exchange was conducted between 200 mL of feed solutions over the seven different applied current densities (0.1, 0.2, 0.5, 1, 2, 5, 10 mA/cm^2). The blue curve represents the measured voltage over time, while the gold triangles represent the measured salinity values of Stream I and II at the beginning and end of a completed salinity exchange process. The applied current density for each run is listed at the top of each subfigure.

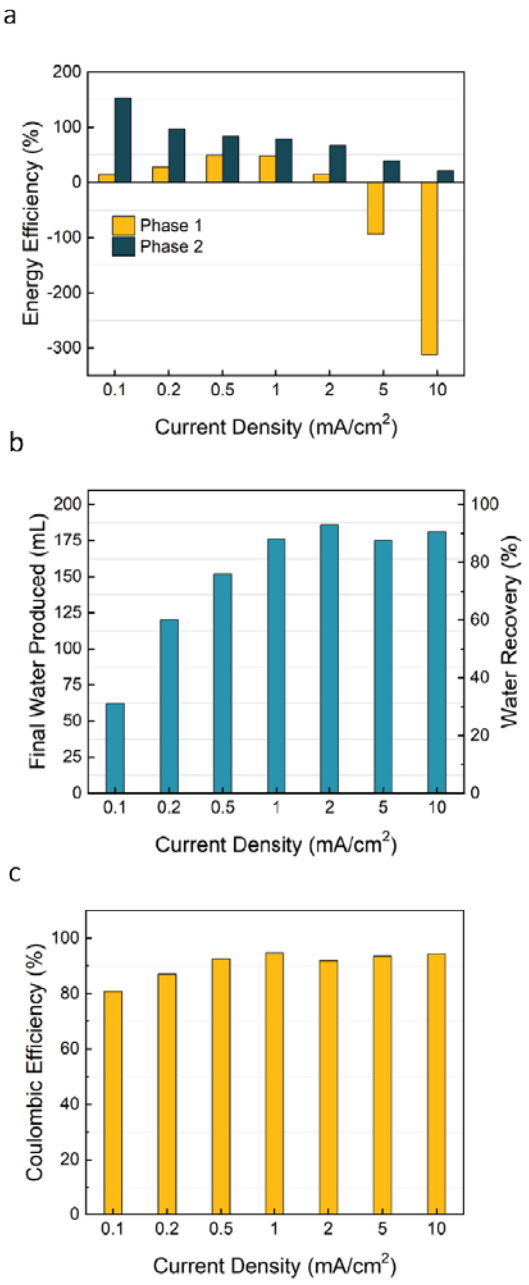

Figure S4. SEE performance under varying current densities. **a**, Energy efficiencies for phases 1 and 2 calculated for varying current densities. The lowest current density resulted the most significant water transport and human error in experiments, leading to a lower calculated energy consumption than the theoretical, shown by the 0.1 mA/cm^2 having a phase 2 energy efficiency above 100%. As shown, both phase 1 and 2 energy efficiencies decrease with increasing current density. The highest current densities (5 & 10 mA/cm^2) resulted in a negative phase 1 energy efficiency because the movement of ions occurred too quickly to observe an energy generation. **b**, Final volume of desalinated water produced for varying current densities. The proportional water recovery percentage is also shown. **c**, Coulombic efficiency over varying current densities.

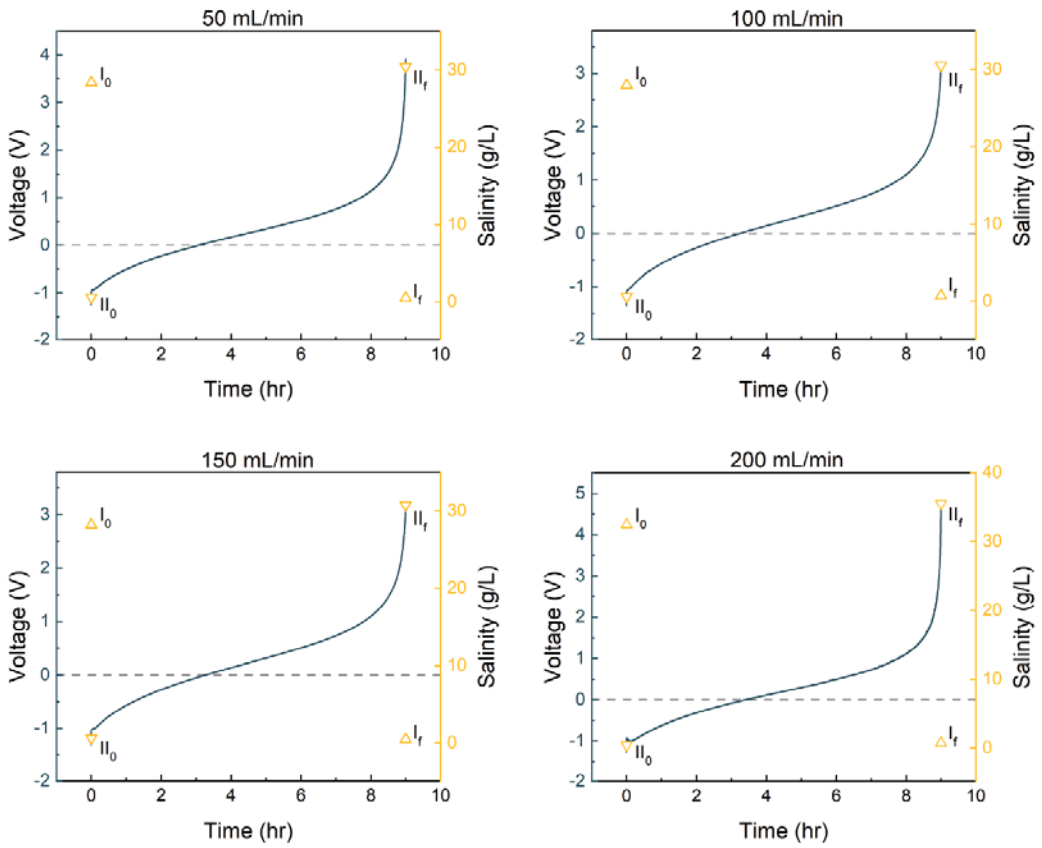

Figure S5. SEE operation for varying circulation flow rates. The operating conditions for varying circulation flow rate were a Stream I NaCl concentration of 0.6 M, a Stream II NaCl concentration of 0.01 M, an applied current density of 1 mA/cm^2, and an operating time of 9 hours. The flow rate for the electrode rinse solution was fixed at 100 mL/min. Salinity exchange was conducted between 200 mL of feed solutions over a range of feed solution flow rates (50-200 mL/min). The blue curve represents the measured voltage over time, while the gold triangles represent the measured salinity values of Stream I and II at the beginning and end of a completed salinity exchange process. The circulation flow rate for each run is listed at the top of each subfigure.

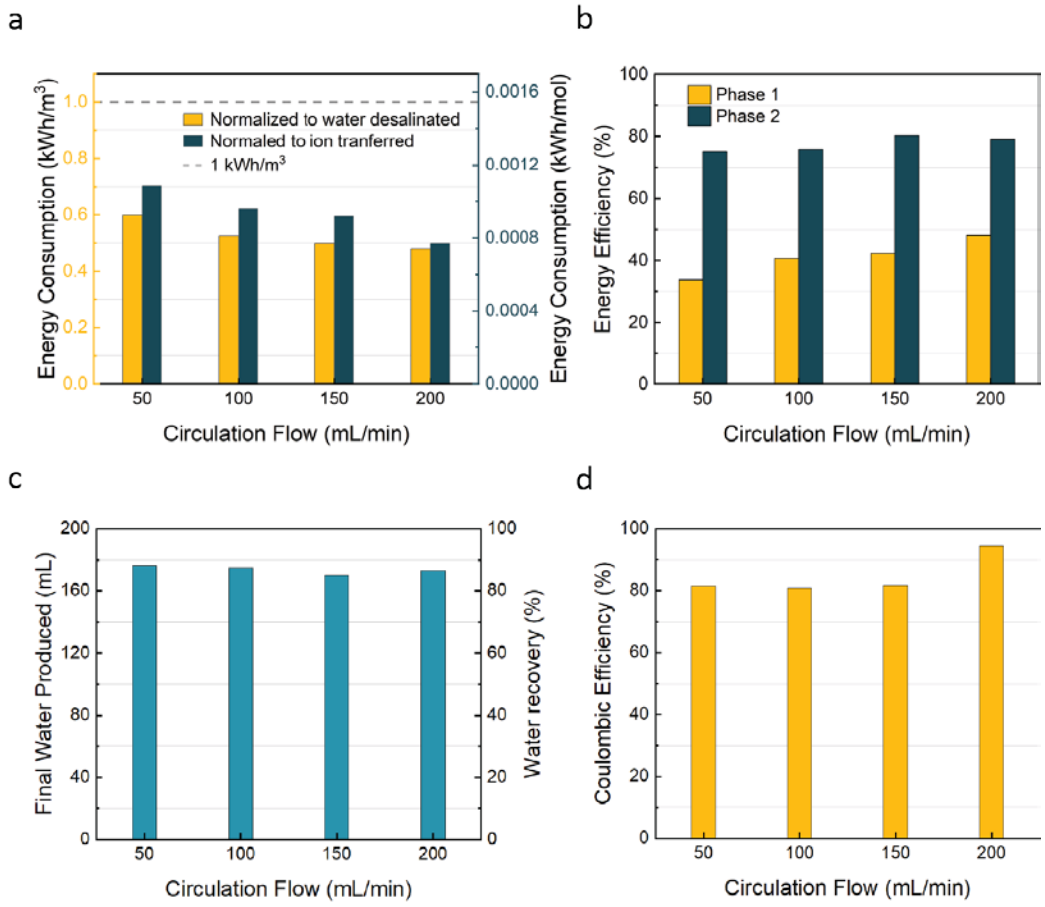

Figure S6. SEE performance with different circulation flow rates. **a**, Energy consumption of the SEE process with various circulation flow rates (50-200 mL/min). This energy analysis does not account for any pumping costs as this was out of the scope for preliminary testing/results of SEE. **b**, Energy efficiency of phases 1 and 2 for different circulation flow rates. **c**, Final volume of desalinated water produced for varying circulation flow rates. The proportional water recovery percentage is also shown. **d**, Coulombic efficiency for varying circulation flow rate.

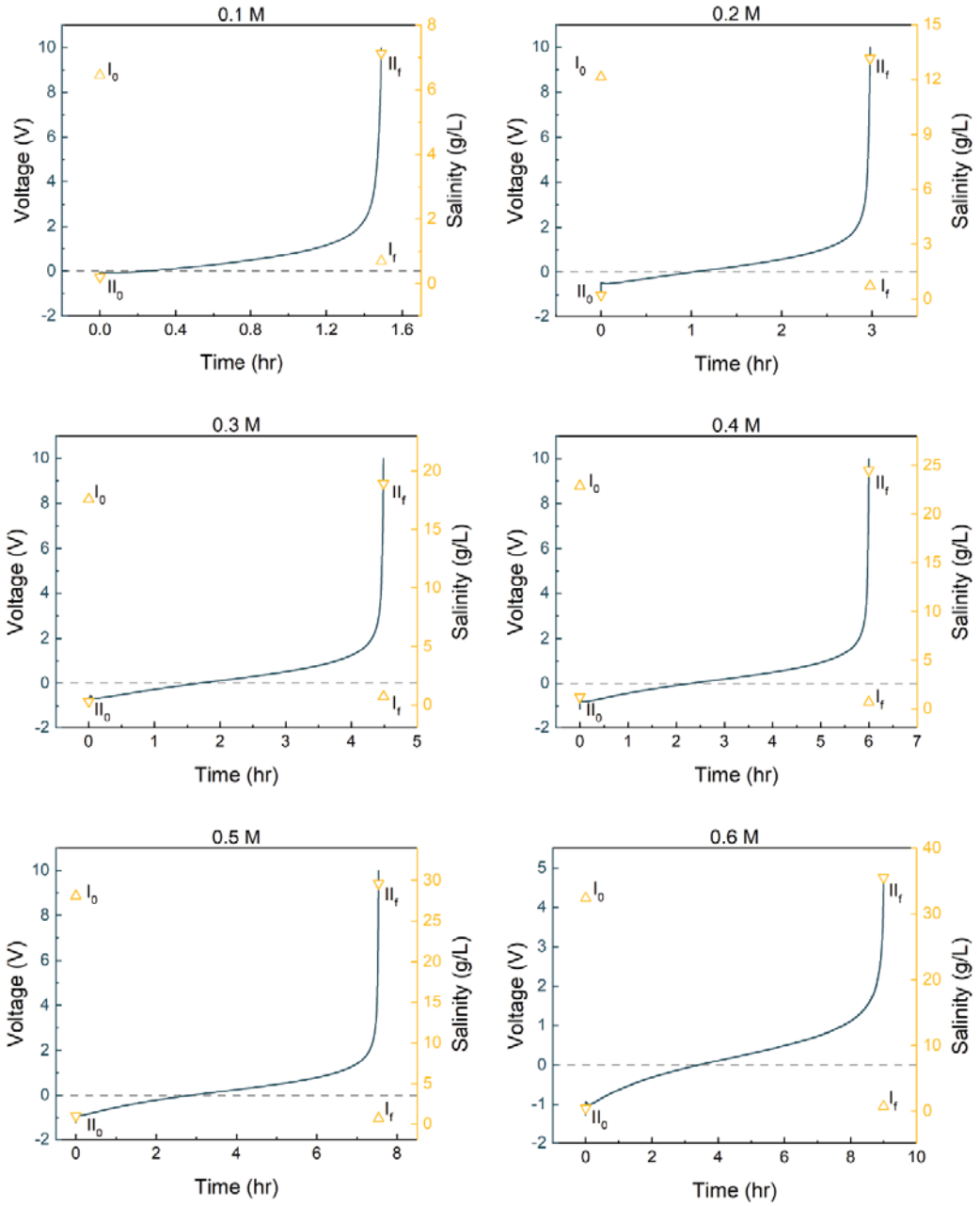

Figure S7. SEE operation for varying NaCl concentration of Stream I. The operating conditions for varying NaCl concentration of Stream I were a feed solution flow rate of 200 mL/min, a Stream II NaCl concentration of 0.01 M, an applied current density of 1 mA/cm^2, and an operating time of 9 hours. The flow rate for the electrode rinse solution was fixed at 100 mL/min. Salinity exchange was conducted between 200 mL of feed solutions over six different initial NaCl concentrations of Stream I (0.1-0.6 M). The blue curve represents the measured voltage over time, while the gold triangles represent the measured salinity values of Stream I and II at the beginning and end of a completed salinity exchange process. The initial NaCl concentration of Stream I for each run is listed at the top of each subfigure.

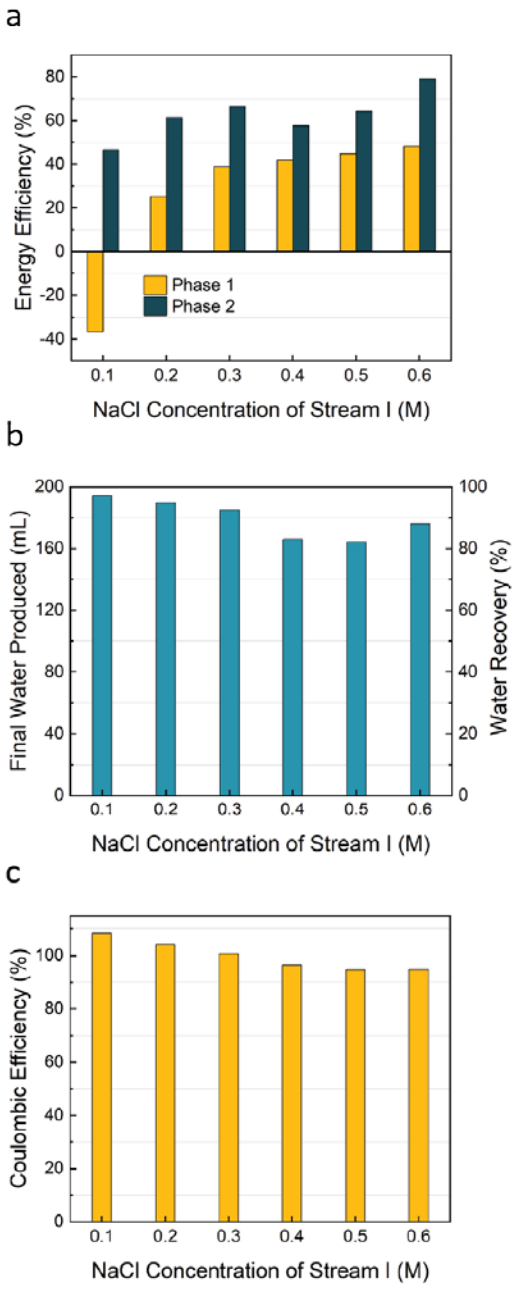

Figure S8. SEE performance over different NaCl concentrations of Stream I. **a**, Energy efficiencies for phases 1 and 2 calculated for varying Stream I NaCl concentrations. As shown, both phase 1 and 2 energy efficiencies decrease with decreasing Stream I concentrations. The lowest Stream I concentration (0.1 M) resulted in a negative phase 1 energy efficiency because there was not enough salinity gradient between Stream I and II to observe an energy generation. **b**, Final volume of desalinated water produced for varying NaCl concentrations of Stream I. The proportional water recovery percentage is also shown. **c**, Coulombic efficiency for varying NaCl concentrations of Stream I.

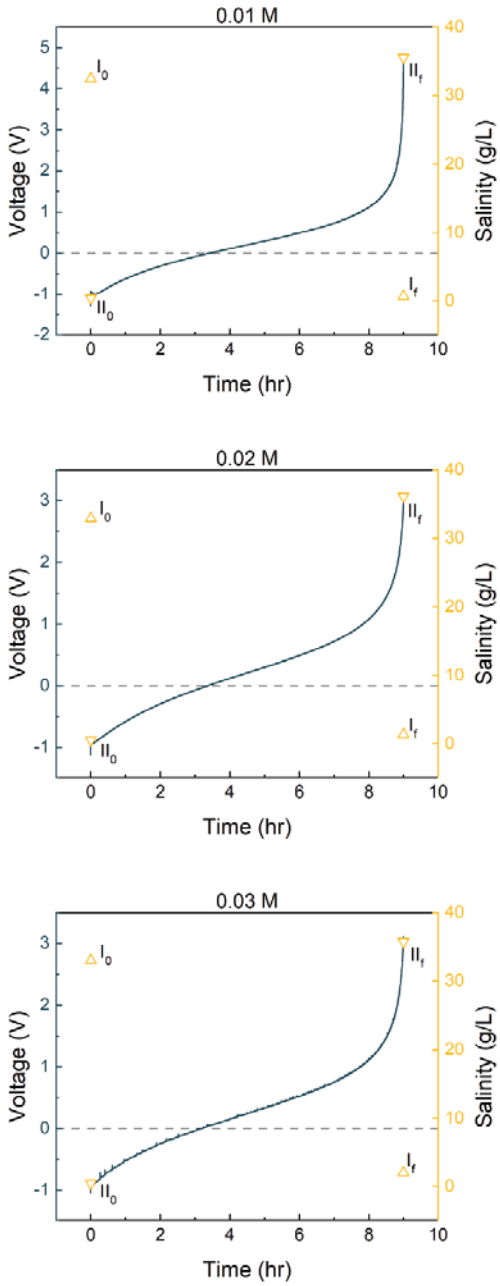

Figure S9. SEE operation for varying NaCl concentration of Stream II. The operating conditions for varying NaCl concentration of Stream II were a feed solution flow rate of 200 mL/min, a Stream I NaCl concentration of 0.6 M, an applied current density of 1 mA/cm^2, and an operating time of 9 hours. The flow rate for the electrode rinse solution was fixed at 100 mL/min. Salinity exchange was conducted between 200 mL of feed solutions over three different initial NaCl concentrations of Stream II (0.01-0.03 M). The blue curve represents the measured voltage over time, while the gold triangles represent the measured salinity values of Stream I and II at the beginning and end of a completed salinity exchange process. The initial NaCl concentration of Stream II for each run is listed at the top of each subfigure.

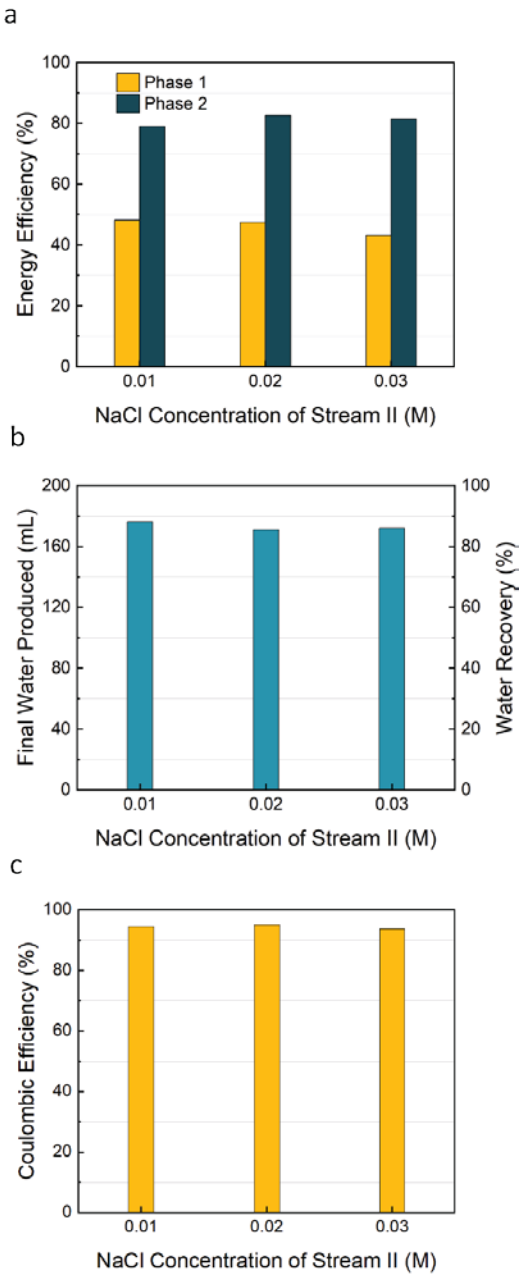

Figure S10. SEE performance over different NaCl concentrations of Stream II. **a**, Energy efficiencies for phases 1 and 2 calculated for varying Stream II NaCl concentrations. **b**, Final volume of desalinated water produced for varying NaCl concentrations of Stream II. The proportional water recovery percentage is also shown. **c**, Coulombic efficiency for varying NaCl concentrations of Stream II.

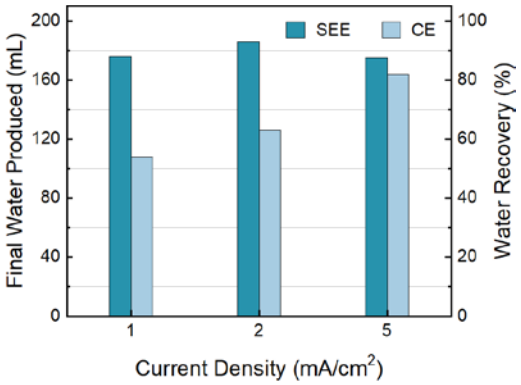

Figure S11. Final volume of desalinated water produced for SEE and conventional electrodialysis (CE) under varying current densities. The proportional water recovery percentage is also shown.

REFERENCES

Brydges T, Lorimer J (1983). The dependence of electro-osmotic flow on current density and time. Journal of Membrane Science, 13(3): 291-305

Galama A H, Saakes M, Bruning H, Rijnaarts H H M, Post J W (2014). Seawater predesalination with electrodialysis. Desalination, 342: 61-69

Indusekhar V, Krishnaswamy N (1985). Water transport studies on interpolymer ion-exchange membranes. Desalination, 52(3): 309-316

Mulder M, Mulder J (1996). Basic principles of membrane technology. Springer Science & Business Media

Porada S, Van Egmond W J, Post J W, Saakes M, Hamelers H V M (2018). Tailoring ion exchange membranes to enable low osmotic water transport and energy efficient electrodialysis. Journal of Membrane Science, 552: 22-30

Ramon G Z, Feinberg B J, Hoek E M V (2011). Membrane-based production of salinity-gradient power. Energy & Environmental Science, 4(11): 4423-4434

Sata T (2007). Ion exchange membranes: preparation, characterization, modification and application. Royal Society of chemistry

Strathmann H (2004). Ion-exchange membrane separation processes. Elsevier

Tedesco M, Hamelers H, Biesheuvel P (2016). Nernst-Planck transport theory for (reverse) electrodialysis: I. Effect of co-ion transport through the membranes. Journal of Membrane Science, 510: 370-381

Tedesco M, Hamelers H, Biesheuvel P (2017). Nernst-Planck transport theory for (reverse) electrodialysis: II. Effect of water transport through ion-exchange membranes. Journal of Membrane Science, 531: 172-182

Turek M (2003). Cost effective electrodialytic seawater desalination. Desalination, 153(1): 371-376

Wilson J R (1960). Demineralization by electrodialysis. Butterworths Scientific Publications